Discriminative and Robust Competitive Code for Palmprint Recognition

Yong Xu, *Senior Member, IEEE*, Lunke Fei, *Student Member, IEEE*, Jie Wen, and David Zhang, *Fellow, IEEE*

***Abstract*—Various palmprint recognition methods have been proposed based on orientation features of palmprints. Among them, the competitive code method using the dominant orientation of palmprint images achieves promising performance in palmprint recognition. In this paper, we propose a discriminative and robust competitive code based method, which uses a more accurate dominant orientation representation of palmprint images for palmprint authentication. Moreover, we propose to weight the orientation information of a neighbor area to improve the precision and stability of the discriminative and robust dominant orientation code. Experiments performed on three types of palmprint databases and a noisy dataset validate the effectiveness of the proposed method.**

***Index Terms*—Biometric, discriminative competitive code (DCC), palmprint recognition, robust orientation extraction.**

I. Introduction

AS A BIOMETRIC trait, a palmprint contains many stable and discriminative features, including not only principal lines and wrinkles but also abundant minutiae and textural features [1]–[3]. Palmprint-based authentication is able to achieve reliable personal verification and identification and it has received increasing research interest in recent years [4]–[6]. Many methods have been proposed to extract different kinds of palmprint features for palmprint recognition [7], [8]. For example, Huang *et al.* [9] extracted the principle lines of palmprints for palmprint verification. Dai *et al.* [10] applied statistics of ridges to design a high-resolution palmprint recognition algorithm. Shen *et al.* [11] used a set of 3-D Gabor filters with different frequencies and orientations to extract spatial and spectrum domain features. In addition, Imtiaz and Fattah [12] proposed a wavelet-based palmprint recognition method by extracting spatial variations from the palmprint image. Roux *et al.* [13] applied a phase-based algorithm to extract corresponding point pairs of a palmprint and Badrinath and Gupta [14] used phase-difference information for palmprint recognition. Further, several minutiae-based feature extraction algorithms were designed for palmprint recognition [15], [16]. Robust point features of a palmprint extracted by the scale invariant feature transform were proposed for contactless palmprint recognition [17]. Jia *et al.* [18] proposed a palmprint-based method using the histogram of oriented lines, which is also robust to the change of illumination of a palmprint. The fusion of different kinds of palmprint features has attracted much research interest [19]. For instance, Li *et al.* [20] designed a palmprint recognition method by fusing the 2-D and 3-D features of palmprint. Xu *et al.* [21] proposed a sparse representation method for bimodal palmprint fusion and recognition. Zhang *et al.* [22] supplied a multispectral palmprint recognition method which captured palmprint images under Red, Green, Blue, and near-infrared light. The four spectral features were fused at the image or matching score level to improve the performance of palmprint identification [23]. Xu *et al.* [24] proposed a more accurate personal identification method by combining the left and right palmprints. In addition to the above methods, subspace-based methods, such as locality preserving projections and linear discriminant analysis [25], [26], and sparse representation-based classification methods, such as collaborate representation classification [27] and two phase test sample sparse representation [28], [29], can also be used for palmprint recognition.

The palmprint is full of lines and textural features which carry rich distinctive orientation information. So the orientation based methods are deemed to be the most promising palmprint recognition methods. Zhang *et al.* [30] first introduced a normalized 2-D Gabor filter to extract a certain orientation feature of palmprint images, namely palmcode. After that, the orientation-based coding methods are successfully developed. In coding based palmprint recognition methods, one or several filters are used to extract palmprint orientation features and these features are converted into digital codes.

The competitive code method [31] is one of the most impressive orientation-based methods. It uses six Gabor filters with different orientations to extract the dominant orientation feature from a palmprint. Six Gabor templates with six orientations [e.g., $j\pi/6(j = 0, 1, \ldots, 5)$] are convoluted with the palmprint image. The dominant orientation is the one that produces the most strong response, and the index $j(j = 0, 1, \ldots, 5)$ of which is taken as the competitive code. The angular distance metric is used to evaluate the distance

Manuscript received May 17, 2016; accepted July 27, 2016. This work was supported by the National Natural Science Foundation of China under Grant 61370163, Grant 61332011, Grant 61501230, and Grant 61572284. This paper was recommended by Associate Editor K. Huang. *(Corresponding author: Yong Xu.)*

Y. Xu, L. Fei, and J. Wen are with the Bio-Computing Research Center, Shenzhen Graduate School, Harbin Institute of Technology, Shenzhen 518055, China (e-mail: laterfall@hitsz.edu.cn; flksxm@126.com; wenjie@hrbeu.edu.cn).

D. Zhang is with the Biometrics Research Centre, Department of Computing, Hong Kong Polytechnic University, Hong Kong (e-mail: csdzhang@comp.polyu.edu.hk).

Color versions of one or more of the figures in this paper are available online at http://ieeexplore.ieee.org.

Digital Object Identifier 10.1109/TSMC.2016.2597291

between two competitive codes. In real operation, the competitive code is usually represented as three binary codes via the rule in [31]. Then, the hamming distance can be used to match two competitive code planes

$$D(P, Q) = \frac{\sum_{i=1}^{N} \sum_{j=1}^{N} \sum_{k=1}^{3} (U_k(i, j) \oplus V_k(i, j))}{3N^2} \quad (1)$$

where $U_k(V_k)$ is the kth bit binary code plane and "$\oplus$" is the bitwise "exclusive OR(xor)" operation. The smaller the hamming distance (or angular distance) is, the more similarity there is between two palmprint images.

Based on the same rule of the dominant orientation extraction, the robust line orientation code (RLOC) method [32] adopts the modified finite radon transform to extract orientation codes. Similarly, the fusion code method [33] uses four complex Gabor filters with orientations of $j\pi/4(j = 0, 1, 2, 3)$ to extract the dominant orientation feature of palmprint images. The phase with the largest magnitude of the four filtering results is converted into a pair of binary codes. Fei *et al.* [34] noted that the most dominant orientation is usually associated with top-two strong filtering responses, and thereby proposed a double orientation code (DOC) method to encode the orientation indices of Gabor filters with the top-two maximum filtering responses. Nevertheless, the orientation with the second maximum filtering response is not always near to the dominant orientation. In addition, to better describe the orientation feature of bend lines in palmprint images, Fei *et al.* [35] divided one Gabor filter into two half-Gabor filters to generate two banks of half-Gabor filters, and then used them to extract two half-orientation codes (HOC) of palmprint images.

To obtain more orientation features, the binary orientation co-occurrence vector (BOCV) method [36] also used six Gabor filters to convolve with palmprint images. Rather than directly extracting all orientation features, Zhang *et al.* [37] extended the BOCV to E-BOCV, in which the fragile bits of BOCV are detected and filtered out. In addition, Sun *et al.* [38] proposed the ordinal code method, in which the orthogonal line ordinal feature of a palmprint is extracted by using three integrated perpendicular 2-D Gaussian filters.

Among all palmprint features mentioned above, the dominant orientation should be the most discriminative orientation feature of a palmprint [31], and the competitive code method is one of the most promising orientation-based coding methods, in which the dominant orientation feature of palmprint images is extracted based on the winner-takes-all rule. It is based on the theory that the filter response reaches the maximum when the filter orientation is consistent with that of the palmprint line. However, in a real operation, the orientations of adopted Gabor filters are discrete. The orientation feature extracted by using discrete orientations of Gabor filters usually only approximates the dominant orientation of a palmprint image. This motivated us to find a more accurate orientation feature representation of palmprint images.

In this paper, a discriminative and robust dominant orientation-based method is proposed, which extracts not only the dominant orientation code of palmprint images but also the side code of the dominant orientation code. Combining the dominant orientation code with the side code can accurately represent the most dominant orientation feature of palmprint images. Further, by weighting the convolution results in orientation extraction, the precision and stability of the dominant orientation feature can be effectively improved. In addition, the number of Gabor filters used in the method is the same as the conventional competitive code method, but it can obtain more accurate dominant orientation features of palmprint images. Extensive experiments performed on public palmprint databases and synthetic noisy dataset demonstrated that the proposed method outperforms the state-of-the-art orientation-based coding methods.

The remainder of this paper is organized as follows. Section II presents a more discriminative and robust competitive code (DRCC) method for orientation representation and recognition of palmprint images. Extensive experiments are carried out and analyzed in Section III. Finally, Section IV concludes this paper.

II. Discriminative and Robust Competitive Code

A. Most Dominant Orientation Feature of Palmprint

The principal orientation feature of a palmprint has been widely used for palmprint recognition. By simply coding the principal orientation feature plane of the palmprint, accurate palmprint recognition can be implemented. In the competitive code method, six Gabor filters with different orientations are used to convolve with palmprint images. The orientation of the filter with the maximum filter response is extracted as the dominant orientation, which is treated as the principal orientation feature of the palmprint. However, in real operation of the dominant orientation extraction, only limited Gabor filters with discrete orientations are used. Thus, the orientation of the filter that has the largest filter response is usually not the exact principal orientation of the palmprint but is very close to it. As shown in Fig. 1, two pixels on a principal line of a palmpirnt are selected to convolve with a set of discrete Gabor filters and the corresponding filtering results are calculated. The orientations with the maximum filter response are then determined as the dominant orientations as shown in Fig. 1, from which it can be seen that the extracted dominant orientations of Fig. 1(a) and (b) are the same, e.g., $\pi/6$. Actually, the genuine principal orientations of these two pixels in Fig. 1(a) and (b) are on the left and right sides of the extracted dominant orientation, respectively. Such observations can also be found on other points of the palmprint. Hence, the dominant orientation extracted based on the maximum response may not accurately represent the principal orientation feature of the palmprint.

The winner-takes-all rule for dominant orientation extraction is based on the underlying assumption that a pixel in a palmprint image belongs to a line [30], [31]. The filter response will reach the maximum when the orientation of the Gabor filter is consistent with the principal orientation of the palmprint. In other words, the Gabor filter response is proportional to the extent of the overlapping between the principal line and filters. However, since limited discrete filters are used in real operations, as shown in Fig. 2, it is possible that no Gabor filter has the same orientation as the principal orientation of the palmprint image. As a result, in this case the extracted orientation cannot accurately represent the

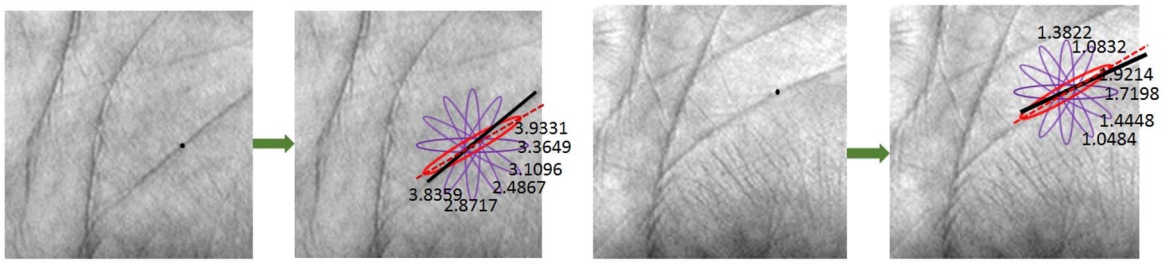

(a) (b)

Fig. 1. Relationship between the genuine principal orientation of a palmprint and the dominant orientation obtained using a set of discrete Gabor filters. (a) and (b) Principal orientation of the palmprint is on the left and right sides of the extracted dominant orientation, respectively.

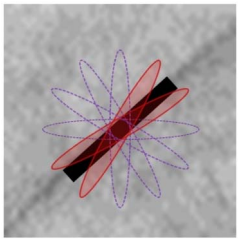

Fig. 2. Illustration of dominant orientation extraction by using six discrete Gabor filters. It is possible that no Gabor filter has the same orientation as the real principal orientation of the palmprint.

principal orientation feature of the palmprint. Intuitively, the Gabor filters, whose orientations are near the exact principal orientation of palmprint, usually have greater filter responses than the others. Therefore, the neighbor orientation of the extracted dominant orientation, which usually also has a larger filter response, can be integrated with the dominant orientation for more accurate representation of palmprint images.

B. Discriminative Competitive Code

In this section, we present the discriminative competitive code (DCC) method. Various filters, including the Gabor filter, Random filter, and Gaussian filter [2], are frequently used to extract orientation features in coding-based methods. Of them, the Gabor filter is the most promising for orientation extraction of images [39] because it has good properties of the 2-D spectral specificity of texture as well as its variation with 2-D spatial position [40]. Xue *et al.* [41] compared the performance of orientation-based palmprint recognition methods by using different filters and concluded that the Gabor filter had better performance than other filters. Therefore, in our method we also use the Gabor filter to extract the orientation features of palmprint images. The Gabor filter has the following general form:

$$G(x, y, \theta, \mu, \sigma, \beta) = \frac{1}{2\pi\sigma\beta}\exp\left[-\pi\left(\frac{x'^2}{\sigma^2}+\frac{y'^2}{\beta^2}\right)\right]\exp\left(i2\pi\mu x'\right) \tag{2}$$

where $x' = (x-x_0)\cos\theta+(y-y_0)\sin\theta$, $y' = -(x-x_0)\sin\theta+(y-y_0)\cos\theta$, (x_0, y_0) is the center of the function, μ is the radial frequency in radians per unit length, θ is the orientation of the Gabor function in radians, and σ and β are the standard deviations of the elliptical Gaussian along the x and y axes, respectively. The ranges of x and y are the sizes of the filter and $i = \sqrt{(-1)}$. Parameters are empirically set as $\mu = 0.0916$, and $\sigma = \beta = 5.6179$ [30]. The real part of the Gabor filter is applied to obtain the orientation feature of a palmprint.

Before feature extraction, the palmprint image is preprocessed to extract the region of interest (ROI) using the method in [33]. For extraction of dominant orientation, six Gabor filters with orientations of $j\pi/6(j = 0, 1, \ldots, 5)$ are used for filtering the palmprint image. The maximum filter response at an orientation is treated as confident features of this orientation [31], [34]. Let G_j be the real part of G with orientation $j\pi/6(j = 0, 1, \ldots, 5)$, which are convolved with the palmprint image by

$$R_j(x, y) = G_j * I(x, y). \tag{3}$$

I is a palmprint image, and "*" is the convolution operation. $R_j(x, y)$ is the filtering response of $I(x, y)$ with G_j. The dominant orientation of point $I(x, y)$ is determined by using the winner-takes-all rule that treats the orientation with the maximum filtering response as the dominant orientation of the palmprint

$$C(x, y) = \arg\max_j R_j(x, y), (j = 0, 1, \ldots, 5) \tag{4}$$

where C is the dominant orientation code of the palmprint image. Let C_{left} and C_{right} represent the two nearest neighbor orientation indices of C on the left and right sides of C, respectively. These two neighbor orientation indices are calculated as follows:

$$C_{\text{left}} = \begin{cases} C+1 & \text{if } 0 \le C \le 4 \\ 0 & \text{if } C = 5 \end{cases} \tag{5}$$

and

$$C_{\text{right}} = \begin{cases} C-1 & \text{if } 1 \le C \le 5 \\ 5 & \text{if } C = 0. \end{cases} \tag{6}$$

Then, the Cs, which represents the "side information" of the obtained dominant orientation of the palmprint image, can be calculated based on the filtering responses of two neighbor orientations. Cs is calculated with the rule of

$$Cs(x, y) = \begin{cases} 1 & \text{if } R_{C_{\text{left}}}(x, y) \ge R_{C_{\text{right}}}(x, y) \\ 0 & \text{otherwise} \end{cases} \tag{7}$$

Cs is referred to as the side code. Since C denotes the dominant orientation feature of palmprint image and Cs indicates

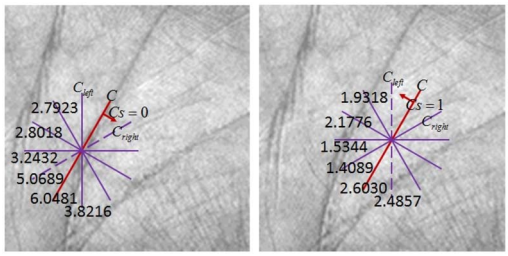

Fig. 3. Procedure for extraction of the winning orientation and side information.

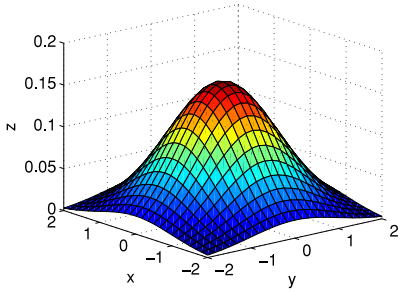

Fig. 4. Shape of the Gaussian weighting template.

the side code of the dominant orientation, combining C and Cs can accurately describe the dominant orientation feature of palmprint images. The conventional competitive code method uses six possible orientations to describe the dominant orientation feature of palmprint images. By contrast, the proposed method adopts 12 possible values to represent the dominant orientation feature of palmprint images. So it is more accurate and discriminative than the conventional competitive code method. The combination of C and Cs, i.e., (C, Cs), is referred to the DCC. An example of calculation of (C, Cs) is depicted in Fig. 3.

C. Extraction of Discriminative and Robust Competitive Code

In the extraction of ROI [30], the palmprint image is aligned based on the gaps between figures and then the center area of a palmprint image is cropped and normalized as the ROI, which inevitably encounters some rotation, translation, and scale variations. In addition, the palmprint images especially those contactless palmprint images usually contain noises. Thus, the DCC of the palmprint image may not robustly and accurately represent the orientation feature of the palmprint image. It is known that the orientation feature of a palmprint is extracted based on the texture of a small area of the palmprint image. In other words, a small area of points in a palmprint image should have similar orientation features. Therefore, the extraction of the orientation feature of a point in a palmprint image should consider the orientation information of the nearby points. This motivated us to use a weighted template to balance the filter results of the palmprint image. Intuitively, a more nearby neighbor of a point should be more related to and contribute more to the orientation feature of the point. Thus, the Gaussian filter is an appropriate choice to weight the contributions of a neighbor area. In general, the Gaussian filter has the following representation:

$$Gs(x, y, \sigma) = \frac{1}{2\pi\sigma^2}\exp\left(-\frac{x^2+y^2}{2\sigma^2}\right) \tag{8}$$

where, σ defines the shape of the Gaussian filter. Since the template should be used in a small area, the size of the Gaussian filter is empirically defined as 5×5, and σ is empirically set to 1. Fig. 4 shows the shape of the Gaussian weighting template.

By using the Gaussian filter template, the Gabor filtering responses of a palmprint image can be smoothed by weighting the original filtering responses of the nearby points via

$$Rb_j(x, y) = Gs * R_j(x, y) \tag{9}$$

where, R_j is the original filtering plane calculated by using (4) and Rb_j is the corrected filtering responses on an orientation of $j\pi/6, j = 1, 2, \ldots, 5$. In real operation, (3) and (9) can be combined to improve the efficiency via

$$Rb_j(x, y) = \bar{G}_j * I(x, y) \tag{10}$$

where $\bar{G}_j = G_j * Gs$. Then, the extraction of the dominant orientation code can be improved based on the weighted filter results by using

$$\tilde{C}(x, y) = \arg\max_j Rb_j(x, y), j = 0, 1, \ldots, 5. \tag{11}$$

Similar to (7), the side code of the dominant orientation code is calculated based on the balanced filtering responses as follows:

$$\tilde{Cs}(x, y) = \begin{cases} 1 & \text{if } Rb_{C_{\text{left}}}(x, y) \geq Rb_{C_{\text{right}}}(x, y) \\ 0 & \text{otherwise.} \end{cases} \tag{12}$$

Since the filter results of the orientation feature of a palmprint image are weighted combination of the nearby points, the dominant orientation feature extracted using (11) and (12) should be more robust than the DCC to the scale, rotation, translation, and noise. The combination of $\tilde{C}$ and $\tilde{Cs}$, i.e., $(\tilde{C}, \tilde{Cs})$, is considered as the DRCC of a palmprint image.

D. Matching

In the matching stage of palmprint images, a similar but not the same angular distance as the competitive code method is used to determine the similarity between two palmprint images X and Y is defined as

$$\begin{aligned} M(X, Y) &= \frac{1}{2N^2}\sum_{i=1}^{N}\sum_{j=1}^{N}\Big[\Big(\tilde{C}_X(i,j) == \tilde{C}_Y(i,j)\Big) \\ &\quad + \Big(\tilde{C}_X(i,j) == \tilde{C}_Y(i,j)\Big) \cap \neg\Big(\tilde{Cs}_X(i,j) \oplus \tilde{Cs}_Y(i,j)\Big)\Big] \end{aligned} \tag{13}$$

where $\tilde{C}_X$ and $\tilde{C}_Y$ are two DRCC planes of X and Y, $\tilde{Cs}_X$ and $\tilde{Cs}_Y$ are the side code planes of $\tilde{C}_X$ and $\tilde{C}_Y$, respectively, and N^2 is the size of the image. The result of operation "==" is 1 if the two codes are the same; otherwise, the result is 0. "$\cap$" is the bitwise "AND" operation, "$\oplus$" is the bitwise "xor" operation, and "$\neg$" is the bitwise "NOT." It can been seen that the range of M is between 0 and 1, and the maximum

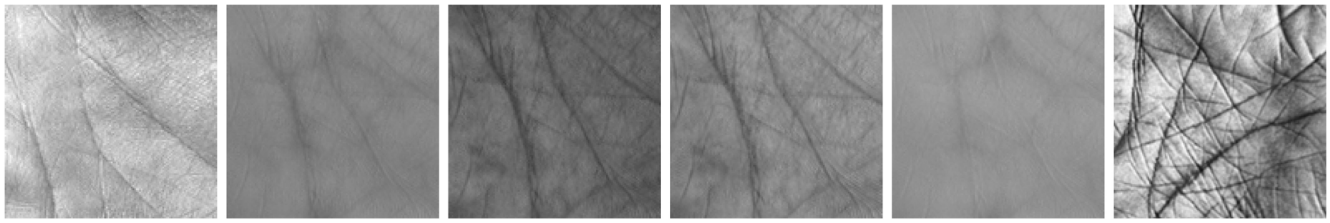

(a) (b) (c) (d) (e) (f)

Fig. 5. ROI images selected from three types of palmprint databases. (a)–(f) Palmprint ROI images selected from the PolyU, Red, Green, Blue, NIR, and IITD databases, respectively.

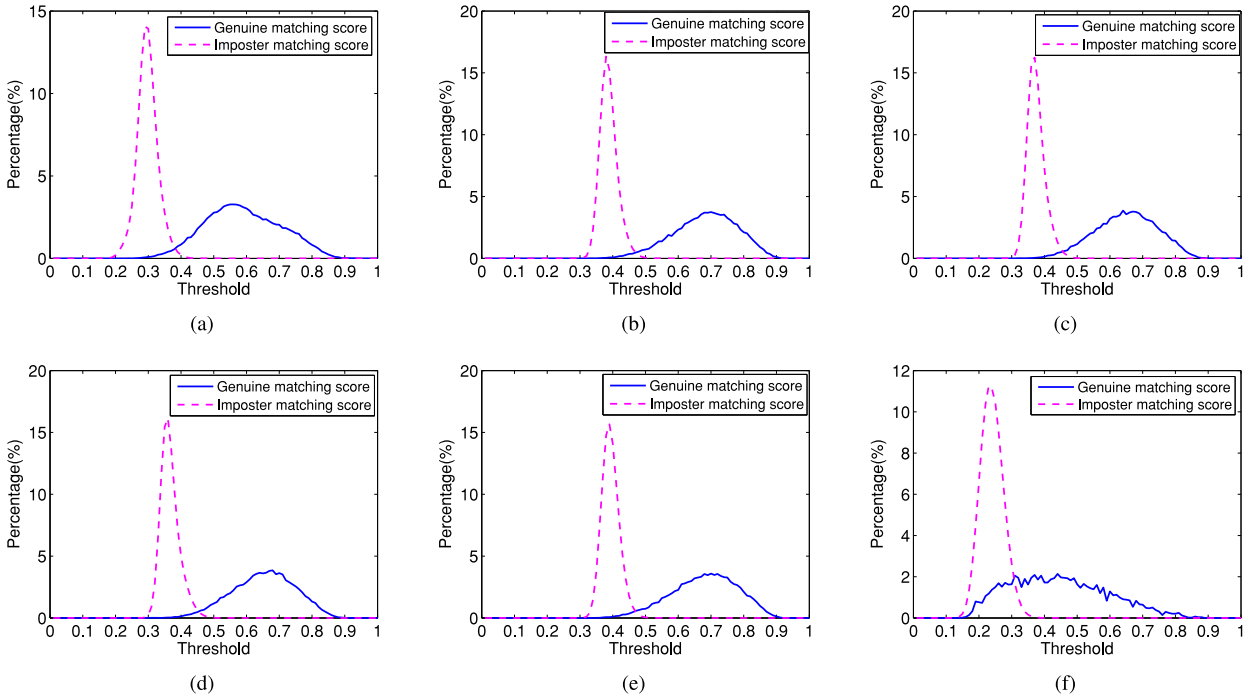

Fig. 6. Matching score distributions obtained using the proposed method. (a)–(f) Distributions of the genuine matching scores and imposter matching scores on the PolyU, Red, Green, Blue, NIR, and IITD databases, respectively.

matching score is 1. The larger the $M(X, Y)$ is, the higher similarity between X and Y is.

It is noted that the matching procedure on two DRCC planes consists of two parts: 1) the dominant orientation code matching and 2) side code matching. The matching score of the dominant orientation codes is directly obtained based on the similarity between them. Nevertheless, two side codes are considered to be matched if these two side codes are the same and the corresponding dominant orientation codes are also the same. Therefore, the matching score of the side code involves the similarity of both the dominant orientation codes and side codes. The matching scores of the dominant orientation codes and side codes are fused to obtain the final matching score of the DRCC.

III. Experiments

A series of experiments are carried out to test the performance of the proposed method on three types of palmprint databases: 1) the PolyU; 2) multispectral; and 3) IITD palmprint databases. Previous state-of-the-art orientation-based methods are compared with the proposed method.

A. Palmprint Database

The PolyU database (version 2) [42] contains 7752 palmprint images collected from 193 individuals. The samples of each individual were collected in two separated sessions and the average interval between the first and second sessions was around two months. About ten palmprint images were captured from both the left and right palm for each individual in each session. So each individual was asked to contribute around 40 palmprint images. The PolyU palmprint database contains 386 classes and each class contains about 20 palmprint images.

The multispectral palmprint database [42] contains four spectrum palmprint databases, the Red, Green, Blue, and Near Infrared (NIR). Each spectrum database was collected from 250 subjects (195 are males and 55 are females) with both of the left and right palms. The age of them was from 20 to 60 years old. The palmprint images were also captured in two separated sessions with an interval of about nine days. In a session, each individual was asked to provide six images for a palm. In summary, a palm contributed 12 images under each illumination. Therefore, each spectral database contains 6000 spectral images from 500 palms.

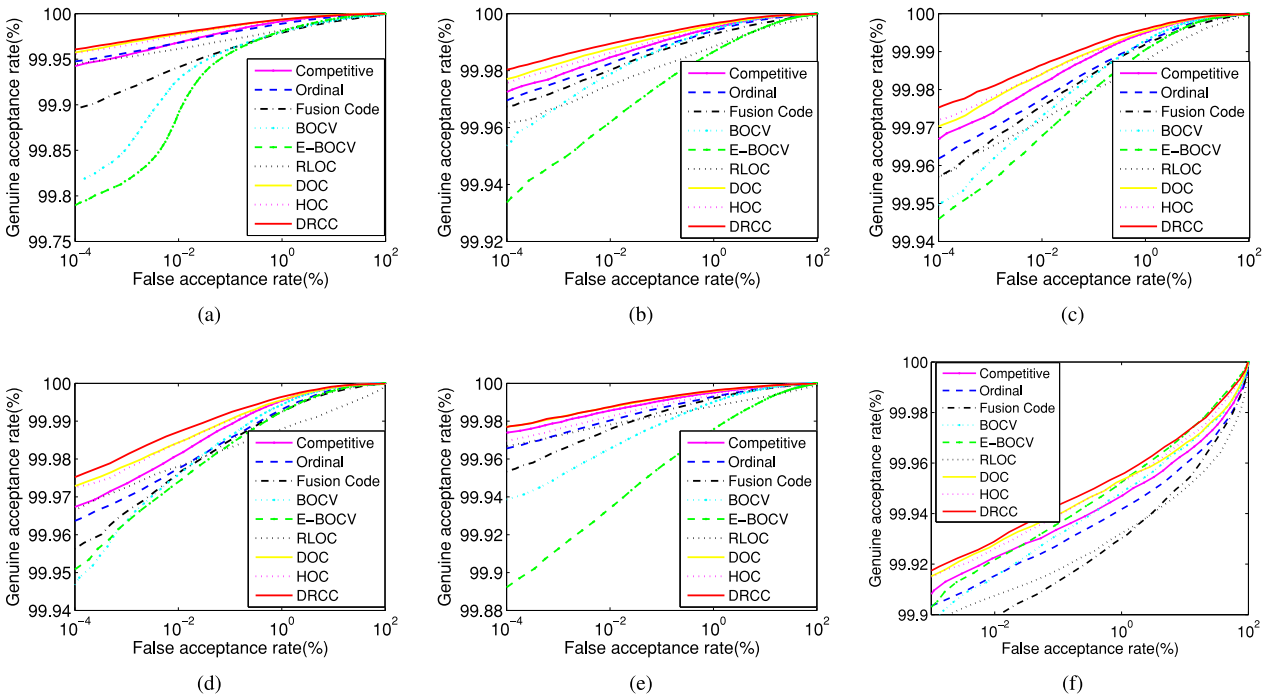

Fig. 7. ROC curves of different methods on different types of databases. (a)–(f) ROC curves on the PolyU, Red, Green, Blue, NIR, and IITD databases, respectively.

TABLE I
EERs (%) OF DIFFERENT METHODS ON THREE TYPES OF PALMPRINT DATABASES

EERs	Competitive code	Ordinal code	Fusion code	BOCV	E-BOCV	RLOC	DOC	HOC	DRCC
PolyU	0.0261	0.0272	0.0899	0.0469	0.0532	0.0360	0.0198	0.0204	**0.0189**
Red	0.0145	0.0161	0.0179	0.0186	0.0131	0.0223	0.0119	0.0131	**0.0104**
Green	0.0168	0.0202	0.0216	0.0232	0.0303	0.0249	0.0146	0.0144	**0.0127**
Blue	0.0170	0.0202	0.0212	0.0207	0.0225	0.0203	0.0146	0.0147	**0.0123**
NIR	0.0137	0.0180	0.0213	0.0284	0.0510	0.0208	0.0121	0.0139	**0.0119**
IITD	0.0696	0.0744	0.0878	0.0708	0.0671	0.0826	0.0622	0.0633	**0.0548**

The public IITD palmprint database [43] is a different palmprint database from the above two databases. The images in the IITD database were captured by a contactless device. Specially, all palmprint images in the IITD database were captured in an relative free environment without using any user-pegs, where the hand are variable in pose, rotation, and translation. Therefore, the database contains intraclass variations. The IITD database contains 2600 hand images from 230 individuals. Five or six palmprint images were captured from each hand of each individual in every session. In experiments, the first five palmprint images from each palm are employed. Thus, there are 460 different palms and each palm has five palmprint images. In the database, all palmprint ROI images have been cropped and then resized to 150 × 150 pixels.

It is seen that different palmprint databases depict different kinds of palmprint images. The PolyU and multispectral palmprint databases characterize the palmprint images under the normal visible light illumination, Red spectrum, Blue spectrum, Green spectrum, and NIR spectrum, respectively. Comparatively, the IITD palmprint database describe the palmprint images of the real-world environment. To show the differences of these palmprints, some typical palmprint ROI images selected from these databases are presented in Fig. 5.

B. Palmprint Verification

In palmprint verification, each palmprint image in the database is compared with each of all other images, respectively. A matching is a really genuine match if both of two compared two samples are from the same palm, otherwise, the matching is a really imposter match. In the PolyU palmprint database, there are 7752 samples, so the total number of matches is 7752*7751/2 = 30 042 876, and of which 74 068 are genuine matches and 29 968 808 are imposter matches. In the multispectral database, each spectral palmprint database has 6000 samples, so there are 6000*5999/2 = 17 997 000 matches, and the genuine matching and imposter matching numbers are 33 000 and 17 964 000, respectively. In the IITD database, there are 4600 genuine matches and 2 369 250 imposter matches.

Fig. 6(a)–(f) shows the distributions of genuine matching score and imposter matching scores obtained using the proposed method on the PolyU, Red, Green, Blue, NIR, and IITD databases, respectively. It can be seen that the genuine

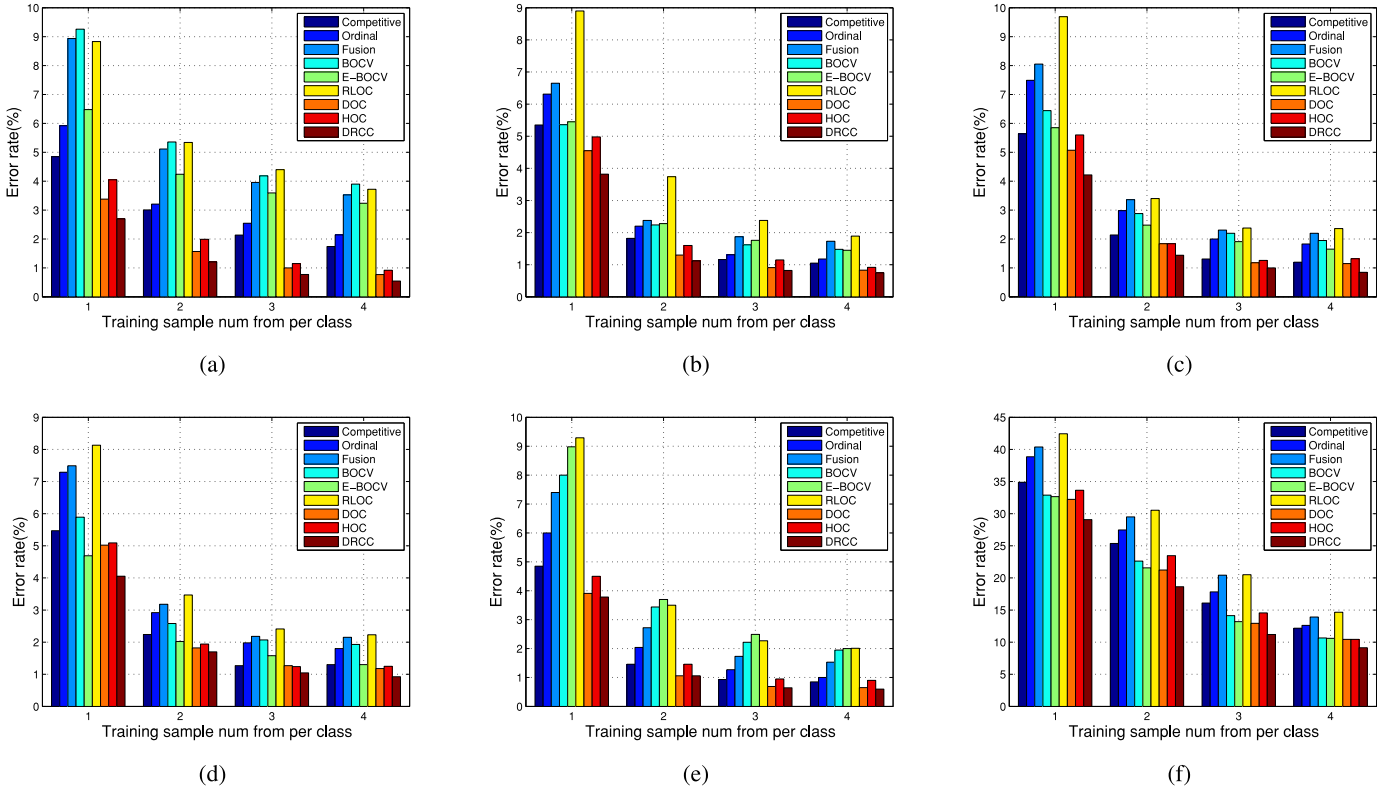

Fig. 8. Palmprint identification error rate. (a)–(f) Error rate of palmprint identification on the PolyU, Red, Green, Blue, NIR, and IITD databases, respectively.

matching score and imposter matching score have highly separate distributions on the PolyU and multispectral databases. The distribution from the IITD database is not as separated as that on the PolyU database. The main reason is that the palmprint images of the same palm in the IITD database are varying owing to rotations and translations. On the other hand, the imposter matching score is also usually smaller than the genuine matching score.

Genuine acceptance rate (GAR) and false acceptance rate (FAR) were used to evaluate the verification performance of the proposed method. The receiver operating characteristic (ROC) curve, which is a graph of GAR versus FAR for all possible decision thresholds, was introduced to compare the performance of different methods. The ROC curves of the proposed method on different palmprint databases are shown in Fig. 7. To facilitate comparison with other methods, ROC curves of the state-of-the-art orientation-based coding methods, including the competitive code, ordinal code, fusion code, BOCV, E-BOCV, RLOC, DOC, and HOC methods, are also shown in Fig. 7. From these ROC curves it can be seen that the proposed method always achieves the highest GAR against the same FAR among all methods.

Equal error rate (EER) is the point where the false reject rate equals to the FAR. The corresponding EER of different coding methods are presented in Table I. It is seen that the proposed method achieves the lowest EER among all methods on all databases. Compared with the conventional competitive code method, the "drop rate of EER" improved by the proposed method is about 27.6% ((0.0261-0.0189)/0.0261) on the PolyU database. For the IITD database, the drop rate of EER is about 21% ((0.0696-0.0548)/0.0696), and the "drop rates of EER" of more than 10% can also be achieved on the multiple spectral databases.

C. Palmprint Identification

Identification is implemented by the procedure of one-against-many comparison which determines the class index of the query sample. In palmprint identification experiments of this paper, the first $N(N = 1, 2, 3, 4)$ palmprint images of each palm are employed as training samples and the remaining palmprint images form the test sample set. Each sample in the test sample set is compared with all samples of each class in the training set to calculate the matching score. The class that produces the highest matching score is treated as the class of the test sample. Previous state-of-the-art coding-based methods, such as the competitive code, ordinal code, fusion code, BOCV, E-BOCV, RLOC, DOC, and HOC methods are compared with the proposed method. In the competitive code method, a small matching score between two palmprint images means high similarity between them. So the class with the smallest competitive code matching score will be selected as the class of the testing sample. Some other coding-based methods, such as the ordinal code, fusion code, BOCV and E-BOCV methods, also use the same rule as the competitive dode method. The experimental results on three types of palmprint databases are shown in Fig. 8. It is seen that the proposed method achieves the lowest identification error rate among all orientation-based methods.

TABLE II
EER(%) OF THE PALMPRINT VERIFICATION OBTAINED USING THE DCC

Database	PolyU	Red	Green	Blue	NIR	IITD
EER	0.0189	0.0107	0.0122	0.0124	0.0117	0.0626

TABLE III
ERROR RATES (%) OF THE PALMPRINT IDENTIFICATION OBTAINED USING THE DCC AND DRCC

Database	PolyU	Red	Green	Blue	NIR	IITD
DCC(N=1)	2.86	4.00	4.51	4.27	3.83	31.79
DRCC(N=1)	**2.70**	**3.81**	**4.22**	**4.05**	**3.78**	**29.08**
DCC(N=2)	1.30	1.28	1.54	**1.64**	**0.98**	21.08
DRCC(N=2)	**1.21**	**1.12**	**1.44**	1.70	1.06	**18.62**
DCC(N=3)	0.79	0.91	**0.98**	1.08	**0.56**	12.38
DRCC(N=3)	**0.77**	**0.82**	1.00	**1.04**	0.64	**11.19**
DCC(N=4)	0.66	0.80	0.93	0.93	**0.55**	9.35
DRCC(N=4)	**0.54**	**0.75**	**0.85**	0.93	0.60	**9.13**

It is noted that both the HOC and DOC methods extract double codes to present the dominant orientation feature of palmprint images. However, the motivations of the HOC and DOC methods are different. The HOC method proposes to extract the orientation feature of bend lines in palmprint images. The double codes of the HOC are extracted independently and thus they can be the same or different values. The DOC method proposes to use two neighbor orientations to capture the dominant orientation feature of palmprint images, and the double codes of the DOC are always different. The commonality of the HOC and DOC methods is that the double codes of them are in the ranges of 1–6. Different from the DOC and HOC methods, our method uses a simple and effective binary side code to accurately denote the real dominant orientation of palmprint images. The comparison results show that the dominant orientation code fusing with the side code outperforms the conventional double code-based methods.

D. Comparison With DCC

To better evaluate the effectiveness of the DRCC, we perform palmprint verification and identification using the DCC. Specifically, we use (C, Cs) calculated by using (4) and (7) to perform palmprint verification and identification. The verification and identification results obtained using the DCC are shown in Tables II and III, respectively. Comparing Table II with Table I, we see that the DCC can achieve similar EER on the PolyU and multispectral databases. However, the EER obtained using the DCC is not as good as that of the DRCC on the IITD database. The main reason is that the IITD is a contactless palmprint database, the palmprint images in which show serious scale, rotation, and translation variations. Therefore, the DRCC shows better robustness than the DCC to the variations of scales, rotation and translation. Table III lists the palmprint identification results obtained using the DCC and DRCC, where the first to fourth rows are the results of using the first 1–4 images per palm as training samples, respectively. It is easy to see that the DRCC method performs better than the DCC in palmprint identification on the PolyU, Red, Green, Blue, and IITD databases in most conditions. It is noted that the DCC can achieve higher identification accuracy than the DRCC on the NIR database. The possible reason is that for the palmprint images in the NIR database the line orientation feature is not very significant. In summary, the weighting scheme in DRCC is effective and the DRCC performs better than the DCC in most cases.

TABLE IV
EER OBTAINED USING DRCC_12 AND DRCC_12_DOMI ON SIX PALMPRINT IMAGE DATABASES

	PolyU	Red	Green	Blue	NIR	IITD
DRCC_12_domi	0.0242	0.0123	0.0139	0.0136	0.0130	0.0610
DRCC_12	0.0220	0.0115	0.0135	0.0129	0.0125	0.0615

E. Effect of the Number of Gabor Filters

In general, using more orientations of Gabor filters can extract more accurate dominant orientation features of palmprint images. In this section, we test the proposed method using 12 orientations (DRCC_12) with the interval of $\pi/12$. In addition, we also test the DRCC_12 without using the side code. In other words, only the dominant orientation code is used in the matching stage, which is referred to DRCC_12_domi. The EERs obtained using both of them are shown in Table IV.

From Table IV, we can draw the following conclusions. First, DRCC_12 performs better than DRCC_12_domi. It demonstrates that the side code indeed improves the performance of palmprint recognition. Second, DRCC_12_domi achieves lower EER than the conventional competitive code method. So using more orientations of filters can extract relatively more accurate dominant orientation feature of palmprint images. Nevertheless, the improvement is limited. One possible reason is that using more Gabor filters means that the orientations of neighbor Gabor filters are very close, and thereby the filtering results of neighbor orientations are very similar. As a result, the dominant orientation with the maximum filtering response becomes sensitive to small rotations, translations and illuminations. Third, though DRCC_12 and DRCC_12_domi use more orientations of filters than DRCC, DRCC outperforms both of them. This demonstrates that the side code of DRCC is more effective than a conventional method using more Gabor filters. In addition, there is no doubt that increasing the number of Gabor filters will increase the computational cost.

F. Experiments on Noisy Palmprint Image Dataset

In order to evaluate the robustness of the DRCC, we perform palmprint recognition on noisy palmprint images. We simulate noisy palmprint images by imposing 2% "salt and pepper" noises on the PolyU database. Fig. 9 shows some noisy palmprint images. We perform palmprint verification and identification on the synthetic noisy dataset. Further, several representative orientation-based coding methods are also tested on the noisy dataset. In Table V, the first row lists the EER, and the rest four rows summarize the identification error rates

TABLE V
PALMPRINT VERIFICATION AND IDENTIFICATION RESULTS ON POLYU DATABASES WITH 2% "SALT & PEPPER" NOISES (%)

Methods	Competitive code	Ordinal code	Fusion code	BOCV	E-BOCV	RLOC	DOC	HOC	DRCC
verification(EER)	0.0456	0.0475	0.0785	0.0607	0.0623	0.0596	0.0416	0.0407	**0.0334**
identification(N=1)	9.41	9.14	20.99	14.80	9.99	9.86	5.97	6.71	**5.81**
identification(N=2)	6.10	5.42	14.21	9.24	6.62	6.41	3.21	3.72	**2.97**
identification(N=3)	4.78	4.23	11.78	7.61	5.69	5.43	2.38	2.73	**2.11**
identification(N=4)	4.16	3.66	10.91	7.07	4.97	4.82	2.00	2.24	**1.71**

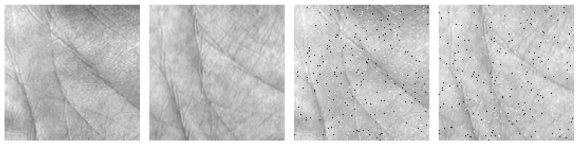

(a) (b) (c) (d)

Fig. 9. Noisy palmprint images. (a) and (b) Original palmprint images. (c) and (d) Noisy palmprint images.

TABLE VI
COMPUTATIONAL COST OF DIFFERENT CODING METHODS

Methods	Feature extraction	Matching	Total
Competitive code	38.670ms	0.077ms	38.747ms
Ordinal code	19.505ms	0.477ms	19.982ms
Fusion code	3.038ms	0.274ms	3.312ms
BOCV	38.224ms	0.987ms	39.211ms
E-BOCV	41.958ms	2.566ms	44.524ms
RLOC	68.871ms	4.242ms	73.114ms
DOC	41.230ms	0.653ms	41.883ms
HOC	48.326ms	0.247ms	48.573ms
DRCC	40.123ms	0.014ms	40.137ms

with using 1–4 images per palm as training samples, respectively. It is seen that the proposed method achieves the lowest EER and error rate of palmprint identification on the noisy dataset.

G. Computational Complexity

To evaluate the computational complexity, we compare the computational time of the proposed method and previous state-of-the-art orientation-based methods. We choose the competitive code, BOCV, E-BOCV, and DOC methods as the baselines for the proposed method uses the similar Gabor filters as these methods. In addition, the ordinal code, fusion code, RLOC, and HOC methods are also implemented for comparison. All methods are implemented using MATLAB 8.1.0 on a PC with configuration of double-core Intel i5-3470 (3.2GHz), RAM 8.00GB, and Windows 7.0 operating system. Both feature extraction and matching of two palmprint images are performed 100 times, and the average time taken in each phase is reported. Table VI summarizes the comparison results, from which we see that the time of feature extraction of the proposed method is about 40.123 ms, which is a little more than that of the competitive code method. The main reason is that it extracts the additional "side code." Due to the simple matching rule, the matching speed of the proposed method is faster than that of the competitive code method. The total computational cost of the proposed method is about 40.137 ms, which is comparable to those baseline methods.

IV. CONCLUSION

Orientation features are frequently and successfully used in coding-based palmprint recognition methods. In this paper, a novel, simple, and efficient DRCC-based method is proposed. The method extracts not only the dominant orientation code but also the side code of palmprint images, and the side code can accurately represent the dominant orientation feature of palmprint images. Furthermore, to improve the robustness, the dominant orientation code and side code are extracted based on the weighting results of Gabor filtering responses in a small neighbor area. To evaluate the performance of the proposed method, three types of palmprint databases, as well as a noisy dataset, are employed. Extensive experiments show that the proposed method can effectively increase the accuracy of palmprint verification and identification in comparison with the state-of-the-art orientation-based methods.

REFERENCES

[1] A. K. Jain, A. Ross, and S. Prabhakar, "An introduction to biometric recognition," *IEEE Trans. Circuits Syst. Video Technol.*, vol. 14, no. 1, pp. 4–20, Jan. 2004.
[2] D. Zhang, *Advanced Pattern Recognition Technologies With Applications to Biometrics*. Hershey, PA, USA: Inf. Sci. Reference, 2009.
[3] Y. Ding, D. Zhuang, and K. Wang, "A study of hand vein recognition method," in *Proc. IEEE Int. Conf. Mechatronics Autom.*, Niagara Falls, ON, Canada, 2005, pp. 2106–2110.
[4] Q. Dai, N. Bi, D. Huang, and F. Li, "M-band wavelets application to palmprint recognition based on texture features," in *Proc. Int. Conf. Image Process. (ICIP)*, Singapore, 2004, pp. 893–896.
[5] F. Yue, B. Li, M. Yu, and J. Wang, "Hashing based fast palmprint identification for large-scale databases," *IEEE Trans. Inf. Forensics Security*, vol. 8, no. 5, pp. 769–778, May 2013.
[6] A. K. Jain and J. Feng, "Latent palmprint matching," *IEEE Trans. Pattern Anal. Mach. Intell.*, vol. 31, no. 6, pp. 1032–1047, Jun. 2009.
[7] D. Zhang, W. Zuo, and F. Yue, "A comparative study of palmprint recognition algorithms," *ACM Comput. Surveys*, vol. 44, no. 1, pp. 2–38, Jan. 2012.
[8] A. Kong, D. Zhang, and M. Kamel, "A survey of palmprint recognition," *Pattern Recognit.*, vol. 42, no. 7, pp. 1408–1418, Jul. 2009.
[9] D.-S. Huang, W. Jia, and D. Zhang, "Palmprint verification based on principal lines," *Pattern Recognit.*, vol. 41, no. 4, pp. 1316–1328, Apr. 2008.
[10] J. Dai, J. Feng, and J. Zhou, "Robust and efficient ridge-based palmprint matching," *IEEE Trans. Pattern Anal. Mach. Intell.*, vol. 34, no. 8, pp. 1618–1632, Aug. 2012.
[11] L. Shen, W. Wu, S. Jia, and Z. Guo, "Coding 3D Gabor features for hyperspectral palmprint recognition," in *Proc. Int. Conf. Med. Biometrics (ICMB)*, Shenzhen, China, 2014, pp. 169–173.
[12] H. Imtiaz and S. A. Fattah, "A wavelet-based dominant feature extraction algorithm for palm-print recognition," *Digit. Signal Process.*, vol. 23, no. 1, pp. 244–258, Jan. 2013.
[13] V. Roux, S. Aoyama, K. Ito, and T. Aoki, "Performance improvement of phase-based correspondence matching for palmprint recognition," in *Proc. IEEE Conf. Comput. Vis. Pattern Recognit.*, Columbus, OH, USA, 2014, pp. 70–77.
[14] G. S. Badrinath and P. Gupta, "Palmprint based recognition system using phase-difference information," *Future Gener. Comput. Syst.*, vol. 28, no. 1, pp. 287–305, Jan. 2012.

[15] E. Liu, A. K. Jain, and J. Tian, "A coarse to fine minutiae-based latent palmprint matching," *IEEE Trans. Pattern Anal. Mach. Intell.*, vol. 35, no. 10, pp. 2307–2322, Oct. 2013.
[16] F. Chen, X. Huang, and J. Zhou, "Hierarchical minutiae matching for fingerprint and palmprint identification," *IEEE Trans. Image Process.*, vol. 22, no. 12, pp. 4964–4971, Dec. 2013.
[17] A. Morales, M. A. Ferrer, and A. Kumar, "Towards contactless palmprint authentication," *IET Comput. Vis.*, vol. 5, no. 6, pp. 407–416, Nov. 2011.
[18] W. Jia, R.-X. Hu, Y.-K. Lei, Y. Zhao, and J. Gui, "Histogram of oriented lines for palmprint recognition," *IEEE Trans. Syst., Man, Cybern., Syst.*, vol. 44. no. 3, pp. 385–395, Mar. 2014.
[19] A. Kumar and S. Shekhar, "Personal identification using multibiometrics rank-level fusion," *IEEE Trans. Syst., Man, Cybern. C, Appl. Rev.*, vol. 41, no. 5, pp. 743–752, Sep. 2011.
[20] W. Li, L. Zhang, D. Zhang, G. Lu, and J. Yan, "Efficient joint 2D and 3D palmprint matching with alignment refinement," in *Proc. IEEE Conf. Comput. Vis. Pattern Recognit. (CVPR)*, San Francisco, CA, USA, 2010, pp. 795–801.
[21] Y. Xu, Z. Fan, M. Qiu, D. Zhang, and J.-Y. Yang, "A sparse representation method of bimodal biometrics and palmprint recognition experiments," *Neurocomputing*, vol. 103, pp. 164–171, Mar. 2013.
[22] D. Zhang, Z. Guo, G. Lu, L. Zhang, and W. Zuo, "An online system of multispectral palmprint verification," *IEEE Trans. Instrum. Meas.*, vol. 59, no. 2, pp. 480–490, Feb. 2010.
[23] R. Raghavendra and C. Busch, "Novel image fusion scheme based on dependency measure for robust multispectral palmprint recognition," *Pattern Recognit.*, vol. 47, no. 6, pp. 2205–2221, Jun. 2014.
[24] Y. Xu, L. Fei, and D. Zhang, "Combining left and right palmprint images for more accurate personal identification," *IEEE Trans. Image Process.*, vol. 24, no. 2, pp. 549–559, Feb. 2015.
[25] J. Gui, W. Jia, L. Zhu, S.-L. Wang, and D.-S. Huang, "Locality preserving discriminant projections for face and palmprint recognition," *Neurocomputing*, vol. 73, nos. 13–15, pp. 2696–2707, 2010.
[26] D. Hu, G. Feng, and Z. Zhou, "Two-dimensional locality preserving projections (2DLPP) with its application to palmprint recognition," *Pattern Recognit.*, vol. 40, no. 1, pp. 339–342, 2007.
[27] L. Zhang, M. Yang, and X. Feng, "Sparse representation or collaborative representation: Which helps face recognition?" in *Proc. IEEE Int. Conf. Comput. Vis. (ICCV)*, Barcelona, Spain, 2011, pp. 471–478.
[28] Y. Xu, D. Zhang, J. Yang, and J.-Y. Yang, "A two-phase test sample sparse representation method for use with face recognition," *IEEE Trans. Circuits Syst. Video Technol.*, vol. 21, no. 9, pp. 1255–1262, Sep. 2011.
[29] Z. Guo, G. Wu, Q. Chen, and W. Liu, "Palmprint recognition by a two-phase test sample sparse representation," in *Proc. Int. Conf. Hand Based Biometrics (ICHB)*, Hong Kong, 2011, pp. 1–4.
[30] D. Zhang, W.-K. Kong, J. You, and L. M. Wong, "Online palmprint identification," *IEEE Trans. Pattern Anal. Mach. Intell.*, vol. 25, no. 9, pp. 1041–1050, Sep. 2003.
[31] A. W.-K. Kong and D. Zhang, "Competitive coding scheme for palmprint verification," in *Proc. Int. Conf. Pattern Recognit. (ICPR)*, Cambridge, U.K., 2004, pp. 520–523.
[32] W. Jia, D.-S. Huang, and D. Zhang, "Palmprint verification based on robust line orientation code," *Pattern Recognit.*, vol. 41, no. 5, pp. 1504–1513, 2008.
[33] A. Kong, D. Zhang, and M. Kamel, "Palmprint identification using feature-level fusion," *Pattern Recognit.*, vol. 39, no. 3, pp. 478–487, 2006.
[34] L. Fei, Y. Xu, W. Tang, and D. Zhang, "Double-orientation code and nonlinear matching scheme for palmprint recognition," *Pattern Recognit.*, vol. 49, pp. 89–101, 2016.
[35] L. Fei, Y. Xu, and D. Zhang, "Half-orientation extraction of palmprint features," *Pattern Recognit. Lett.*, vol. 69, pp. 35–41, Jan. 2016.
[36] W. Zuo, Z. Lin, Z. Guo, and D. Zhang, "The multiscale Competitive Code via sparse representation for palmprint verification," in *Proc. IEEE Conf. Comput. Vis. Pattern Recognit. (CVPR)*, San Francisco, CA, USA, 2010, pp. 2265–2272.
[37] L. Zhang, H. Li, and J. Niu, "Fragile bits in palmprint recognition," *IEEE Signal Process. Lett.*, vol. 19, no. 10, pp. 663–666, Oct. 2012.
[38] Z. Sun, T. Tan, Y. Wang, and S. Z. Li, "Ordinal palmprint representation for personal identification," in *Proc. IEEE Comput. Soc. Conf. Comput. Vis. Pattern Recognit.*, vol. 1. San Diego, CA, USA, Jun. 2005, pp. 279–284.
[39] J. H. V. Deemter and J. M. H. D. Buf, "Simultaneous detection of lines and edges using compound Gabor filters," *Int. J. Pattern Recognit. Artif. Intell.*, vol. 14, no. 6, pp. 757–777, Jun. 2000.
[40] T. S. Lee, "Image representation using 2D Gabor wavelets," *IEEE Trans. Pattern Anal. Mach. Intell.*, vol. 18, no. 10, pp. 959–971, Oct. 1996.
[41] F. Xue, W. Zuo, K. Wang, and D. Zhang, "A performance evaluation of filter design and coding schemes for palmprint recognition," in *Proc. Int. Conf. Pattern Recognit. (ICPR)*, Tampa, FL, USA, 2008, pp. 1–4.
[42] PolyU Palmprint Database (Version 2.0). *Multispectral Palmprint Database*. [Online]. Available: http://www.comp.polyu.edu.hk/∼biometrics/
[43] *IITD Touchless Palmprint Database (Version 1.0)*. [Online]. Available: http://www4.comp.polyu.edu.hk/∼csajaykr/IITD/Database_Palm.htm

Yong Xu (SM'15) received the B.S., M.S., and Ph.D. degrees in pattern recognition and intelligence system from the Nanjing University of Science and Technology, Nanjing, China, in 1994, 1997, and 2005, respectively.

He is currently with the Bio-Computing Research Center, Shenzhen Graduate School, Harbin Institute of Technology, Shenzhen, China. His research interests include pattern recognition, biometrics, bioinformatics, machine learning, image processing, and video analysis.

Lunke Fei (S'15) received the B.S. and M.S. degrees in computer science and technology from East China Jiaotong University, Nanchang, China, in 2004 and 2007, respectively. He is currently pursuing the Ph.D. degree in computer science and technology with the Shenzhen Graduate School, Harbin Institute of Technology, Shenzhen, China.

His research interests include biometrics, pattern recognition, and image processing.

Jie Wen received the M.S. degree from Harbin Engineering University, Harbin, China, in 2015. He is currently pursuing the Ph.D. degree in computer science and technology with the Shenzhen Graduate School, Harbin Institute of Technology, Shenzhen, China.

He has published over ten journal and conference papers. His current research interests include image and video enhancement, pattern recognition, and machine learning.

David Zhang (F'08) received the graduation degree in computer science from Peking University, Beijing, China, the M.Sc. degree in computer science and the Ph.D. degree from the Harbin Institute of Technology (HIT), Harbin, China, in 1982 and 1985, respectively, and the second Ph.D. degree in electrical and computer engineering from the University of Waterloo, Waterloo, ON, Canada, in 1994.

From 1986 to 1988, he was a Post-Doctoral Fellow with Tsinghua University, Beijing, and an Associate Professor with the Academia Sinca, Beijing. He is currently the Head of the Department of Computing, and the Chair Professor with Hong Kong Polytechnic University, Hong Kong, where he is the Founding Director of the Biometrics Technology Centre supported by the Hong Kong SAR Government in 1998. He also serves as a Visiting Chair Professor with Tsinghua University, and an Adjunct Professor with Peking University, Shanghai Jiao Tong University, Shanghai, China, HIT, and the University of Waterloo. He has authored over ten books and 200 journal papers. He is the Founder and an Editor-in-Chief of the *International Journal of Image and Graphics*, the Book Editor of the Springer International Series on Biometrics, an Organizer of the International Conference on Biometrics Authentication, an Associate Editor of over ten international journals, including the IEEE TRANSACTIONS and *Pattern Recognition*.

Prof. Zhang is a Croucher Senior Research Fellow, the Distinguished Speaker of the IEEE Computer Society, and a Fellow of the International Association for Pattern Recognition.